Crystal field effects and thermoelectric properties of $PrFe_4Sb_{12}$ skutterudite

E. Bauer, St. Berger, Ch. Paul, M. Della Mea, G. Hilscher, H. Michor, M. Reissner, and W. Steiner
Institut für Festkörperphysik, Technische Universität Wien, A-1040 Wien, Austria

A. Grytsiv and P. Rogl
Institut für Physikalische Chemie, Universität Wien, A-1090 Wien, Austria

E. W. Scheidt
Lehrstuhl für Experimentalphysik III, Universität Augsburg, D-86159 Augsburg, Germany
(Received 5 August 2002; published 31 December 2002)

Transport and magnetic properties are reported for ternary skutterudites $La_{0.83}Fe_4Sb_{12}$ and $Pr_{0.73}Fe_4Sb_{12}$. Physical properties of $Pr_{0.73}Fe_4Sb_{12}$ are dominated by crystal electric field effects, yielding in the magnetic triplet Γ_5 as ground state. As a result, long-range magnetic order appears below 4.6 K. $Pr_{0.73}Fe_4Sb_{12}$ exhibits an unusually high electronic contribution to the specific heat C_p/T of several hundred mJ/mol K^2, and a significant value of a nuclear Schottky contribution is derived below about 1 K, primarily related to ^{141}Pr with a nuclear spin $I=5/2$. The figure of merit at room temperature, expressing the thermoelectric performance of $Pr_{0.73}Fe_4Sb_{12}$, is about 0.075.

DOI: 10.1103/PhysRevB.66.214421 PACS number(s): 75.40.Cx, 71.27.+a, 71.70.Jp, 71.70.Ch

I. INTRODUCTION

Ternary skutterudites $R_yM_4X_{12}$, with R=rare earth, M=Fe, Co, Rh, Ru, . . . , and X=P, As, Sb, have attracted much interest because of a variety of possible ground states and because of their large thermoelectric potential. Depending on the particular rare earth element, features like superconductivity, such as, e.g., in $LaRu_4As_{12}$ below $T_c=10.3$ K or $LaOs_4As_{12}$ below $T_c=3.2$ K,[1] long-range magnetic order in $EuFe_4Sb_{12}$ at $T_{mag}=84$ K,[2,3] heavy fermion behavior in $YbFe_4Sb_{12}$,[4] non-Fermi-liquid behavior in $CeRu_4Sb_{12}$,[5] intermediate and mixed valence behavior in $Yb(Fe,Co)_4Sb_{12}$ and $Eu(Fe,Co)_4Sb_{12}$,[6,7] and hopping conductivity in $YbRh_4Sb_{12}$,[6] were already found and discussed in some detail. Significant interest in this family of compounds, however, stems from the fact that skutterudites are potential candidates for thermoelectric applications. Materials considered for such use should exhibit values for the *figure of merit* $ZT=S^2T/(\rho\lambda)$ at least of the order of 1 (T=temperature, S=Seebeck coefficient, ρ=electrical resistivity, and λ=thermal conductivity). Depending on the carrier concentration of a particular skutterudite, Seebeck values above about 100 μV/K are frequently observed. Besides, ternary skutterudites are outstanding with respect to their low thermal conductivity which, in some cases, may be near to the theoretical limit. As a matter of fact, the dramatically diminished $\lambda(T)$ values are associated with an exceptionally large thermal displacement parameter of the loosely bound rare earth elements, corresponding to a ''rattling'' (i.e., soft phonon mode) of these atoms in an oversized cage.[8]

Previous studies of Pr-based skutterudites evidenced also a number of remarkable characteristics. Among them is superconductivity in $PrRu_4As_{12}$ and $PrRu_4Sb_{12}$ below 2.4 and 1 K, respectively,[9,10] and a metal to insulator transition in $PrRu_4P_{12}$ at $T_{MI}=60$ K,[11] as well as ordering at $T_{mag}=6.2$ K in $PrFe_4P_{12}$.[12] Kondo-like anomalies in transport phenomena were found for the latter and C_p/T for $T\rightarrow 0$ shows a huge value of about 1.4 J/mol K^2.[13,14] Moreover, de Haas–van Alphen measurements evidenced extraordinary heavy electrons and unusual features of the Fermi surface topology,[15] suggesting strongly correlated electrons in this compound. Recent studies devoted to $PrFe_4P_{12}$,[16,17] however, revealed that the order parameter below 6.4 K is nonmagnetic, most likely of quadrupolar origin. Very recently, heavy fermion superconductivity was discovered in $PrOs_4Sb_{12}$ with a transition temperature of 1.8 K. Specific heat studies suggest that the superconducting ground state is formed from heavy quasiparticles as concluded from a normal-state Sommerfeld value γ of about 500 mJ/mol K^2.[18]

The aim of the present work is to evaluate the ground-state properties of $Pr_{0.73}Fe_4Sb_{12}$ and to explore its thermoelectric potential. Special emphasis is directed to crystal electric field effects which determine low-temperature magnetic and transport properties. In particular, Pr as non-Kramers ion in a cubic environment can result in both a magnetic or a nonmagnetic ground state. For a purpose of comparison, a number of bulk properties derived for isomorphous $La_{0.83}Fe_4Sb_{12}$ are added. Preliminary low-temperature properties concerning $Pr_{0.73}Fe_4Sb_{12}$ are reported in Ref. 19 and the various aspects of stability and crystal chemistry of ternary RFe_4Sb_{12} are discussed in Ref. 2 together with some physical properties.

II. EXPERIMENT

A. Synthesis and x-ray powder diffraction

Starting materials of the title compounds were ingots of La and Pr (99.9 wt %), pieces of iron (99.9 wt %) and rods of antimony (99.9 wt %). Due to the high vapor pressure of Sb at elevated temperatures, arc melting was performed under current as low as possible with repeated melting. With this method and compensating the losses of evaporation by additional Sb a dense product was achieved. The compounds were then sealed under vacuum in silica capsules, slowly heated (50°/h) to a 650 °C, and kept there for up to 150 h followed by quenching in water.

X-ray powder diffraction data were obtained using a Huber-Guinier powder camera applying monochromatic Cu $K\alpha 1$ radiation with an image plate recording system. Lattice parameters were calculated by least-squares fits to the indexed 4θ values applying the program package STRUKTUR (Ref. 20) on the base of our single-crystal data of $YbFe_4Sb_{12}$.[21] For quantitative refinement of the atom positions, the x-ray intensities were analyzed employing the FULLPROF program.[22]

B. Measurements of bulk properties

A superconducting quantum interference device (SQUID) and a vibration magnetometer served for the determination of the magnetization from 2 K up to 300 K in fields up to 6 and 15 T, respectively. Pieces from the bulk specimen (0.15 and 0.17 g, respectively) were used in this study. Specific heat measurements on samples of about 1–2 g were performed at temperatures ranging from 1.5 K up to 120 K by means of a quasi-adiabatic step heating technique in external fields up to 9 T. Specific heat data were also collected at temperatures down to about 100 mK in a $^3He/^4He$ cryostat using a relaxation method.[23]

The electrical resistivity and magnetoresistivity of bar shaped samples (about $1\times1\times5$ mm^3) were measured using a four-probe dc method in the temperature range from 0.4 K to room temperature and fields up to 12 T. A resistivity study of $Pr_{0.73}Fe_4Sb_{12}$ for a few values of externally applied magnetic fields was performed in the $^3He/^4He$ cryostat at temperatures as low as 30 mK employing an ac technique.

A piston-cylinder cell with a Teflon cap and a paraffin mixture as pressure transmitter served to generate hydrostatic pressure up to about 16 kbar. The absolute value of the pressure was determined from the superconducting transition temperature of lead.[24]

Thermopower measurements were carried out with a differential method. The absolute thermopower $S_x(T)$ was calculated using the following equation: $S_x(T)=S_{Pb}(T)-V_{Pb/x}/\Delta T$ where S_{Pb} is the absolute thermopower of lead and $V_{Pb/x}$ is the thermally induced voltage across the sample, depending on the temperature difference ΔT.

Thermal conductivity measurements were performed in a flow cryostat on cuboid-sphaped samples (length about 1 cm, cross section about 2 mm^2), which where kept cold by anchoring one end of the sample onto a thick copper panel mounted on the heat exchanger of the cryostat. The temperature difference along the sample, established by electrical heating, was determined by means of a differential thermocouple (Au+0.07% Fe/Chromel). The measurement was carried out under high vacuum and three shields mounted around the sample reduced the heat losses due to radiation at finite temperatures. The innermost of these shields was kept on the temperature of the sample via an extra heater.

III. RESULTS AND DISCUSSION

A. Structural chemistry

The obtained x-ray intensity pattern, shown in Fig. 1 for $Pr_{0.73}Fe_4Sb_{12}$, was indexed on the base of a body-centered-cubic lattice prompting isotypism with $LaFe_4P_{12}$.[25] The refinement of the x-ray intensities converged satisfactorily for a fully ordered atom arrangement $Pr_yFe_4Sb_{12}$ with respect to atom site distribution among Pr, Fe, and Sb atoms [$Im\bar{3}$, Sb in 24 g, $x_{Sb}=0$, $y_{Sb}=0.1598(1)$, $z_{Sb}=0.3348(1)$, $R_I=0.039$]. Occupation factors were refined and correspond to a full occupancy of the Fe and Sb sublattices but reveal considerable voids for the Pr site accounting for only 73% filling of the rare earth site [$y=0.73(2)$]. The lattice parameter is found to be $a=9.1369(2)$ Å. The corresponding values for $La_yFe_4Sb_{12}$ are $y=0.83$ and $a=9.1471$ Å. Besides the skutterudite phase, traces of Sb (about 3%) were obtained.

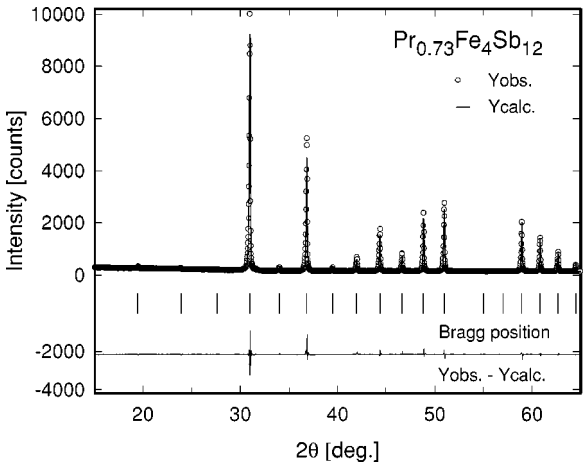

FIG. 1. X-ray pattern of $Pr_{0.73}Fe_4Sb_{12}$.

B. Bulk properties

To initially characterize the magnetic state of $Pr_{0.73}Fe_4Sb_{12}$, dc and ac susceptibility $\chi_{dc}(T)$ and $\chi_{ac}(T)$ measurements were performed. Results are shown in Figs. 2(a) and 2(b). The Curie-Weiss-like behavior at elevated temperatures ($T>50$ K) reveals an effective magnetic mo-

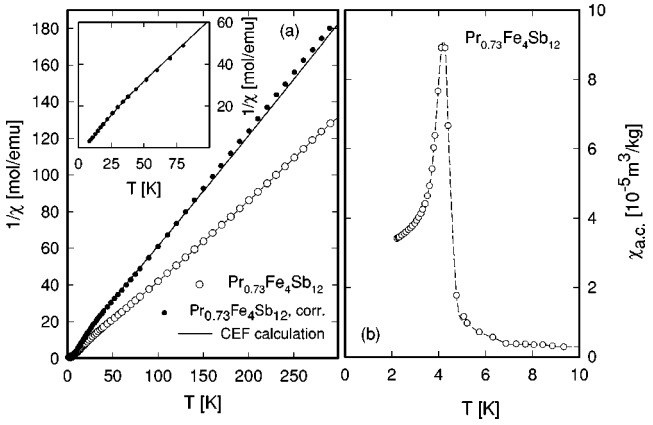

FIG. 2. (a) Temperature-dependent magnetic susceptibility χ of $Pr_{0.73}Fe_4Sb_{12}$ plotted as χ^{-1} vs T. The solid circles represent the Pr-related susceptibility and the solid line is a least-squares fit according to Eq. (2). The inset shows the low-temperature behavior in more detail. (b) $\chi_{ac}(T)$ of $Pr_{0.73}Fe_4Sb_{12}$.

ment $\mu_{eff}=4.19\mu_B$, as well as a paramagnetic Curie temperature $\theta_p \approx 0.5$ K. These paramagnetic quantities are slightly smaller than those reported previously by Danebrock *et al.*[2] In order to match the theoretical rare earth moments associated with a 3+ state of the Pr ion, a significant contribution to μ_{eff} of the $[Fe_4Sb_{12}]$ sublattice is required. Assuming that both the rare earth and the $[Fe_4Sb_{12}]$ contribution to μ_{eff} are simply additive, i.e.,

$$\mu_{eff}^{meas}=\sqrt{y(\mu_{eff}^{Pr})^2+(\mu_{eff}^{[Fe_4Sb_{12}]})^2} \tag{1}$$

(y is the void filling factor), yields an effective magnetic moment for $[Fe_4Sb_{12}]$ of $2.7\mu_B$. Isomorphous compounds $LaFe_4Sb_{12}$ and $CaFe_4Sb_{12}$ (Ref. 2) exhibit effective moments of $\mu_{eff}=3.0\mu_B$ and $\mu_{eff}=3.7\mu_B$, respectively, that primarily have to be attributed to the magnetic behavior of Fe. The assumption that Fe in $Pr_{0.73}Fe_4Sb_{12}$ carries a magnetic moment differs distinctly from the results for isostructural $PrFe_4P_{12}$, the latter point at an effective magnetic moment, perfectly matching the theoretical Pr^{3+} value.[12] A preliminary investigation carried out on $PrCo_4Sb_{10}Sn_2$ yielded $\mu_{eff}=3.63\mu_B$,[26] evidencing the absence of a moment bearing a $[Co_4Sb_{10}Sn_2]$ sublattice in this compound. Binary Co_4Sb_{12} is known to be a diamagnetic semiconductor. These various results imply some exceptional position of the Fe-Sb units with respect to their magnetic properties in filled skutterudites.

Electronic band structure calculations performed for rare-earth-based skutterudites, in particular for $LaFe_4P_{12}$ (Ref. 27) and $LaFe_4Sb_{12}$ (Ref. 28), revealed much narrower valence and conduction bands for the latter due to a significantly larger lattice constant (about 15%). In addition, a double-peak structure of the Fe d partial density of states (DOS) below the Fermi energy E_F in $LaFe_4Sb_{12}$ backs the probability that Fe carries a magnetic moment, in agreement with the experimental evidence by Danebrook *et al.*[2] Preliminary spin-polarized calculations for $LaFe_4Sb_{12}$ also support a magnetic solution.[28] These band structure calculations evidence similar features within a certain family of skutterudites, except the $4f$ contribution when proceeding through the series of rare earths. Assuming that the DOS of $PrFe_4Sb_{12}$ resembles nearly that of $LaFe_4Sb_{12}$, the magnetic moment ascribed to $[Fe_4Sb_{12}]$ follows from a distinct feature of the Fe $3d$ partial DOS around E_F.

A closer inspection of the low-temperature data and of the ac measurement [Fig. 2(b)] indicates an onset of long-range magnetic order. Defining the transition temperature of $Pr_{0.73}Fe_4Sb_{12}$ in a standard manner, i.e., by taking the extremum in $d\chi_{dc}T/dT$,[29] as well as the temperature at half height of the ac susceptibility anomaly on the paramagnetic side reveals $T_{mag} \approx 4.6$ K. The sharp transition and the overall behavior of $\chi_{ac}(T)$ does not exclude a ferromagnetic ground state.

In order to elucidate the above conclusion, isothermal magnetization measurements below and above the transition temperature are shown in Fig. 3. Magnetization curves taken below the ordering temperature [Fig. 3(a)] and even Arrott plots [Fig. 3(b)] do not unambiguously validate ferromagnetism. The magnetization at 2 K and 15 T reaches a value of about $2.6\mu_B$, well below the theoretical saturation magnetization $M_s=3.2\mu_B$. The lower figure is primarily associated with crystalline electric field (CEF) effects, lifting the ground-state degeneracy of the total angular momentum of Pr^{3+}.

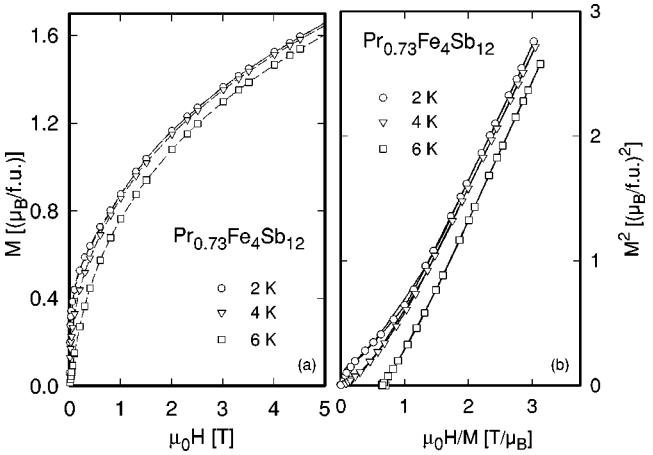

FIG. 3. (a) Isothermal magnetization of $Pr_{0.73}Fe_4Sb_{12}$ at $T=2$, 4, and 6 K. (b). Arrott plots for $Pr_{0.73}Fe_4Sb_{12}$.

The influence of the CEF on the ground-state degeneracy of the Pr ion essentially depends on the crystal symmetry of the compound. Neglecting the impact of vacancies in the Pr sublattice of $Pr_{0.73}Fe_4Sb_{12}$, the cubic symmetry is responsible for a splitting of the $j=4$ total angular momentum of Pr^{3+} into a Γ_1 singlet, a Γ_3 doublet, and in the Γ_4 and Γ_5 triplets. For non-Kramers ions like Pr, nonmagnetic ground states, i.e., Γ_1 and Γ_3, are possible.

To derive some estimate of the particular CEF scheme in $Pr_{0.73}Fe_4Sb_{12}$, an attempt was made to account for the experimentally observed temperature dependent magnetic susceptibility. To fix the contribution originated by Pr, the susceptibility associated with $[Fe_4Sb_{12}]$ is subtracted from the total measured set of data assuming a simple Curie behavior and taking into account $\mu_{eff}([Fe_4Sb_{12}])=2.7\mu_B$. The thus modified $1/\chi(T)$ curve is added in Fig. 2(a).

The susceptibility $\chi(T)$ related to Pr in $Pr_{0.73}Fe_4Sb_{12}$ is analyzed in terms of

$$1/\chi=1/\chi_{CEF}-\lambda, \tag{2}$$

where χ_{CEF} is the susceptibility due to crystal field effects and λ is the molecular field parameter caused by exchange interactions between the Pr ions. When a magnetic field is applied along the direction α, χ_{CEF} follows from the Van Vleck formula[30]

$$\chi_\alpha^{CEF}=\frac{N_A(g_j\mu_B)^2}{\sum_n \exp(-E_n/k_BT)}\sum_{r,s}|\langle r|J_\alpha|s\rangle|^2 \times \exp\left(\frac{-E_r}{k_BT}\right)\frac{\exp[(E_r-E_s)/k_BT]-1}{E_r-E_s}. \tag{3}$$

N_A is the Avogadro number, E_r is the energy of the rth state, g_j is the Landé factor, and $\langle r|J_\alpha|s\rangle$ is the matrix element between the r and s states of a CEF scheme.

Incorporating the CEF Hamiltonian for cubic systems,

$$H_{cub}=B_4^0(O_4^0+5O_4^4)+B_6^0(O_6^0-21O_6^4) \tag{4}$$

(B_n^m are CEF parameters and O_n^m are Stevens operators), and considering the Pr total angular momentum $j=4$ allows the calculation of $\chi_{CEF}(T)$ as well as of $\chi(T)$ by adjusting B_4^0, B_6^0, and λ. Since the present experimental data are derived from polycrystalline material, a uniform susceptibility contribution from the various directions is assumed in the fitting procedure.

A recent reexamination of the CEF for cubic point groups, however, revealed a new nonvanishing term $(O_6^2-O_6^6)$ for the point groups T_h and T due to the lack of umklappung and fourfold symmetry axis of the point group O_h.[31] The degeneracy of each sublevel does not change in comparison to results derived by Eq. (4), but some eigenfunctions and eigenvalues may alter slightly.

In absence of inelastic neutron scattering results and in lack of single crystal data, as well as to keep the number of adjustable parameters low, the term $(O_6^2-O_6^6)$ is omitted in the present investigation for simplicity. A reasonable fit of the experimental data is then obtained for $B_4^0=0.04$ K and $B_6^0=0.001\,33$ K, while the molecular field constant is derived as $\lambda=6$ mol/emu. Results of the calculation are shown in Fig. 2(a) as a solid line. In particular, the pronounced curvature in $1/\chi(T)$ around 25 K is well reproduced [compare inset, Fig. 2(a)] and the overall susceptibility behavior matches fairly well the experiment. Slight differences can also be caused by an inaccurate determination of the Pr contribution. The set of parameters $B_4^0=0.04$ K and $B_6^0=0.001\,33$ K for Pr $j=4$ in cubic symmetry reveals the triplet Γ_5 as ground state, followed by the singlet Γ_1 at 28 K, and again a triplet (Γ_4) at 136 K. The uppermost level is the doublet Γ_3 at 215 K. Associated with the Γ_5 triplet ground state is a magnetic moment of $\mu=2\mu_B$. This finding is consistent with the occurrence of magnetic order and moreover explains the magnitude of the isothermal magnetization at $T=2$ K.

Magnetization measurements performed up to 15 T are an additional possibility to consider crystal field effects and to corroborate the set of the CEF parameters chosen. Plotted in Fig. 4 is the temperature-dependent magnetization for various values of applied magnetic fields. The solid lines are calculations of the magnetization based on Eq. (4) with $g_j=4/5$, $j=4$, $B_4^0=0.04$ K, and $B_6^0=0.001\,33$ K, revealing reasonable agreement with the experimental data. Note that there is no extra adjustable parameter used in this calculation. Although the effective magnetic moment of $[Fe_4Sb_{12}]$ is large, magnetization can be rather small, as a consequence and characteristic feature of itinerant moments. Such a contradictory feature of delocalized moments is well known in the literature, e.g., from the phenomenological Rhodes-Wohlfart plot (compare, e.g., Ref. 32). Both CEF parameters derived above will also serve for a discussion and a satisfactorily description of the specific heat and electrical resistivity observed for $Pr_{0.73}Fe_4Sb_{12}$.

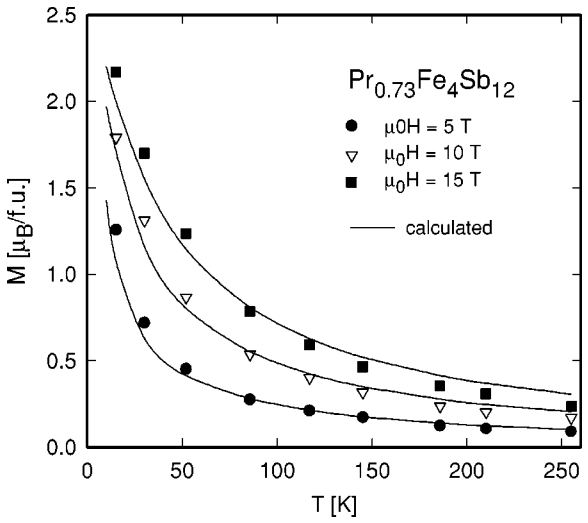

FIG. 4. (a) Temperature-dependent magnetization of $Pr_{0.73}Fe_4Sb_{12}$ for various values of externally applied magnetic fields. The solid lines are theoretical values (see text).

A heat capacity study of $Pr_{0.73}Fe_4Sb_{12}$ was performed from 0.1 to about 30 K in external magnetic fields up to 9 T. Results are shown in Fig. 5 as C_p/T vs T. A pronounced anomaly around 5 K indicates the onset of long-range magnetic order, in agreement with magnetic measurements. By taking the maximum negative slope of $C_p(T)$, the ordering temperature is found to be about 4.5 K. As the field strength increases, the anomaly in $C_p(T)$ becomes washed out, and eventually vanishes for external fields higher than 3 T. In general, such an observation is referred to some anisotropy of the phase boundary in the H vs T plane. At each field value, however, the low-temperature heat capacity is remarkably high. The electronic contribution to the specific heat

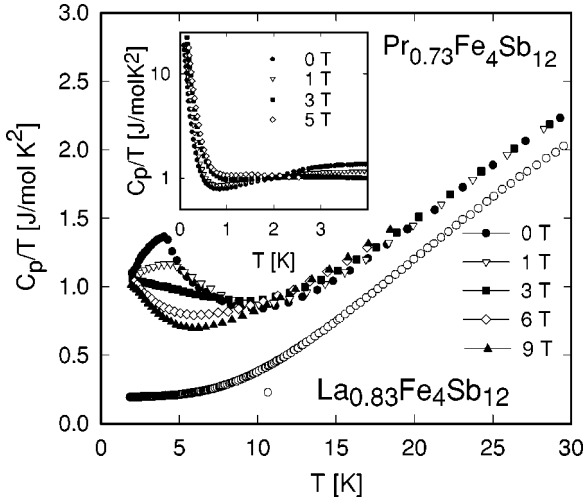

FIG. 5. (a): Temperature- and field-dependent specific heat C_p of $Pr_{0.73}Fe_4Sb_{12}$ and $La_{0.83}Fe_4Sb_{12}$ plotted as C_p/T vs T. The inset shows the low-temperature behavior of $Pr_{0.73}Fe_4Sb_{12}$.

C_p/T thus amounts to several hundred mJ/mol K^2. Such significant values of C_p/T are well known in heavy fermion systems based on Ce, Yb, or U, but were already found in isomorphous Pr compounds as well. For the purpose of comparison $C_p(T)$ of $La_{0.83}Fe_4Sb_2$ is added in this figure. It should be noted that the large γ value observed for $La_{0.83}Fe_4Sb_{12}$ is in convincing agreement to the one calculated from band structure results, mainly referring to the Fe $3d$ contribution.[28]

The inset of Fig. 5 shows the very-low-temperature specific heat behavior of $Pr_{0.73}Fe_4Sb_{12}$ for magnetic fields up to 5 T. C_p/T exhibits a significant rise due to the nuclear heat capacity primarily associated with the $I=5/2$ state of Pr. This is referred to a strong intrasite hyperfine coupling between the nuclei and $4f$ electrons.

To quantitatively account for such a hyperfine contribution to the heat capacity, derived from Fe^{57}, Sb^{121}, Sb^{123}, and Pr^{141}, an average magnetic field and Zeeman splitting is assumed. The best fit of the low-temperature upturn results in a local field of approximately 87 T, but takes only into account 7.3% of all nuclei. One can therefore conclude that the main contribution to the hyperfine term is only due to one kind of nuclei. Assuming a local magnetic field of 73 T at the Pr site, and a slightly enhanced average magnetic field compared to the external field on all the other nuclei sites, fits the data very well. The strong internal field thus derived presumably refers to the Pr vacancies (about 27%) in the skutterudite structure.

At temperatures slightly above the pronounced nuclear contribution ($\approx$1 K), C_p/T increases with external magnetic fields. Fluctuations of the order parameter prior to a field-induced phase transition or the destroying of the ordered state by the magnetic field are well known to cause such an enhancement. A similar field-dependent trend of C_p/T can be found in $PrFe_4P_{12}$.[16]

In order to estimate the characteristic temperature scale for the observed heavy quasiparticles we adopted the resonance level model (RLM) as introduced by Schotte and Schotte[33] and successfully applied by Aoki *et al.*[16] to a related problem in the case of $PrFe_4P_{12}$. This model assumes a narrow Lorentzian density of states at the Fermi energy E_F with a width $\Delta \sim T_K$, where the Kondo temperature T_K is supposed to represent the appropriate temperature scale which describes thermal excitations in a strongly renormalized quasiparticle band formed around E_F. In absence of magnetic fields, specific heat follows from[33]

$$C_{mag}=k_B\frac{2S\Delta}{\pi k_BT}-2k_B\left\{\frac{\Delta^2}{(2\pi k_BT)^2}\left[(2S+1)^2\psi'\times\left(1+\frac{\Delta}{2\pi k_BT}(2S+1)\right)-\psi'\left(1+\frac{\Delta}{2\pi k_BT}\right)\right]\right\}, \tag{5}$$

where S represents an arbitrary impurity spin and ψ is the derivative of the digamma function. A least-squares fit of Eq. (5) to the experimental data, together with the low-temperature phonon contribution derived from $La_{0.8}Fe_4Sb_{12}$ ($C_{ph}^{lt}\approx\beta T^3$, $\beta=0.0008$ J/mol K^4), is displayed in Fig. 6 as a solid line, yielding $T_K\approx 25$ K. The adjustment of T_K is made such to satisfy the entropy balance associated with the phase transition. The results of the RLM show that the jump in the specific heat δ_c at the transition temperature is much smaller than expected, e.g., in a mean-field-like description. Such a reduction, however, is well known in magnetically ordered Kondo lattices where δ_c continuously diminishes as T_K increases with respect to the magnetic interaction strength.[34] An alternate possibility for the rather broad phase transition as evidenced by the specific heat data could be the incomplete filling of the voids at the $2a$ sites of the skutterudite structure. However, ac susceptibility results [compare Fig. 2(b)] reveal a rather sharp phase transition.

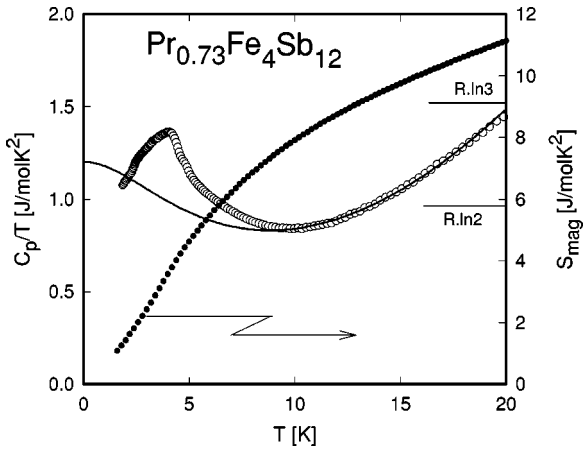

FIG. 6. Temperature-dependent specific heat C_p/T (open circles, left axis) and magnetic entropy (solid circles, right axis) of $Pr_{0.73}Fe_4Sb_{12}$. The solid line is a fit according to the RLM (see text).

The magnetic entropy S_{mag} is derived by a comparison with $La_{0.83}Fe_4Sb_2$. Results of $S_{mag}(T)$ are shown in Fig. 6, right scale. Some inaccuracy of $S_{mag}(T)$ may arise from the different void-filling factor in the case of the Pr-based skutterudite with respect to the isomorphous La skutterudite. In general, the magnetic entropies associated with the itinerant moments of [Fe_4Sb_{12}] sum up to zero at the ordering temperature and have no contribution above T_{mag}. The ground-state degeneracy of the Pr ion is lifted either by magnetic ordering and/or possibly by Kondo interaction, responsible for the large effective electron masses. The entropy release is found to be $R\ln 2$ at about 7 K and $R\ln 3$ around 13 K. Invoking the set of CEF parameters as derived for the analysis of the magnetic susceptibility data reveals an entropy value of $S_{mag}=10$ J/mol K at $T=15$ K, almost in perfect agreement with the experiment, independently backing the derived CEF scheme, where the Γ_5 triplet is the ground state and a nonmagnetic singlet state is situated about 30 K above.

Transport coefficients, i.e., the electrical resistivity ρ, thermopower S, and the thermal conductivity λ, are necessary in order to classify materials as possible candidates for thermoelectric applications. Furthermore, temperature-dependent resistivity measurements allow one to account for existing crystal field influences, making a comparison with the above-derived CEF parameters possible.

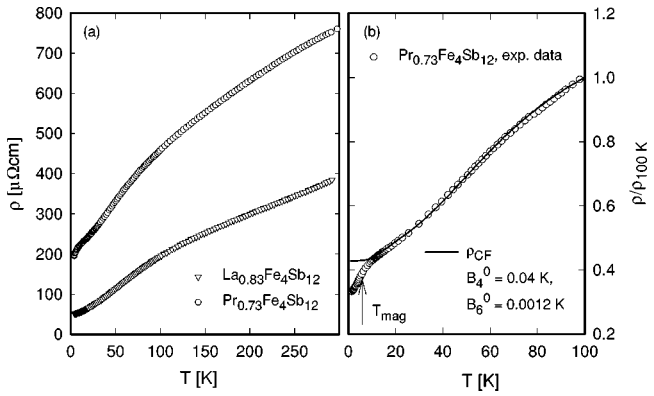

FIG. 7. (a) Temperature-dependent electrical resistivity ρ of $La_{0.83}Fe_4Sb_{12}$ and $Pr_{0.73}Fe_4Sb_{12}$. (b) Normalized resistivity of $Pr_{0.73}Fe_4Sb_{12}$. The solid line represents the CEF derived spin disorder resistivity with $B_4^0 = 0.04$ K and $B_6^0 = 0.001\,33$ K.

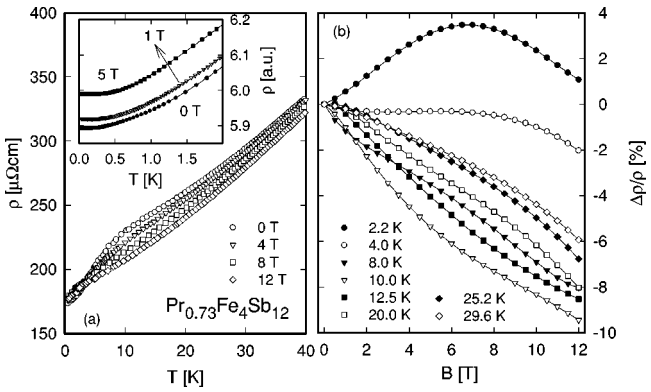

FIG. 8. (a) Temperature- and field-dependent electrical resistivity ρ of $Pr_{0.73}Fe_4Sb_{12}$. The inset shows $\rho(T,B)$ of $Pr_{0.73}Fe_4Sb_{12}$ at very low temperatures. (b) Isothermal magnetoresistance $\Delta\rho/\rho$ of $Pr_{0.73}Fe_4Sb_{12}$.

Shown in Fig. 7(a) is the temperature-dependent electrical resistivity $\rho(T)$ of $Pr_{0.73}Fe_4Sb_{12}$ as well as of $La_{0.83}Fe_4Sb_{12}$. Both compounds behave metallic; i.e., $\rho(T)$ increases with rising temperature. The particular temperature dependence, however, deviates significantly from a simple metal, even in the case of $La_{0.83}Fe_4Sb_{12}$, where La does not carry a magnetic moment. The absolute resistivity values are characteristic for materials having a reduced number of charge carriers. At low temperatures, the weak anomaly in $Pr_{0.73}Fe_4Sb_{12}$ indicates the onset of long-range magnetic order at 4.6 K.

To account for the strongly curved $\rho(T)$ behavior of $Pr_{0.73}Fe_4Sb_{12}$, at least in the lower-temperature range ($T < 100$ K), we attempted to consider the spin disorder resistivity ρ_{spd}, i.e., scattering of conduction electrons on disordered magnetic moments, in combination with CEF effects. According to Ref. 35, ρ_{spd} should read

$$\rho_{spd}(T) = \text{const} \times m^* \mathcal{J}^2 (g_j - 1)^2 \times \sum_{m_s, m_s', i, i'} \langle m_s' i' | \vec{s}\vec{j} | m_s i \rangle^2 p_i f_{ii'}, \qquad (6)$$

where m^* is the effective carrier mass and $\mathcal{J}$ is the s-f coupling constant; m_s and m_s' are the spins of the conduction electrons (holes) in the initial and final states and i and i' are the CEF states with energies E_i and E_i'. The matrix elements are between the simultaneous eigenstates for the local-moment conduction-electron system. $p_i = \exp[-E_i/k_BT]/\Sigma_j \exp[-E_j/k_BT]$ and $f_{ii'} = 2/(1+\exp\{-[(E_i - E_i')/k_BT]\})$. Note that in absence of CEF splitting $\rho_{spd}(T)$ becomes constant. A temperature-independent spin disorder contribution is also expected from scattering on the paramagnetic moments of $[Fe_4Sb_{12}]$.

Using the already derived CEF parameters $B_4^0 = 0.04$ K and $B_6^0 = 0.001\,33$ K, the normalized spin disorder contribution to the electrical resistivity can be calculated without any further free parameters. Results of this calculation are shown in Fig. 7(b), together with the resistivity data of $Pr_{0.73}Fe_4Sb_{12}$ normalized to 100 K. Except at low temperatures, where $Pr_{0.73}Fe_4Sb_{12}$ exhibits a phase transition ($T_{mag} = 4.6$ K), the peculiar structure of $\rho(T)$ is well reproduced by this choice of CEF parameters, already used to trace $\chi(T)$ of $Pr_{0.73}Fe_4Sb_{12}$ over a broad range of temperature. This coincidence can be considered as further hint for the proper choice of the crystal field level scheme, dominated by a magnetic triplet as ground state. Moreover, the phonon contribution to $\rho(T)$ seems not to be of significant importance below 100 K.

Crystal field splitting thus appears to play a dominant role in the series of Pr-based skutterudites. A survey of already studied $PrRu_4Sb_{12}$ (Ref. 10), $PrFe_4P_{12}$ (Ref. 16), $PrOs_4Sb_{12}$ (Ref. 18) and $PrRu_4P_{12}$ (Ref. 36) reveals that the Γ_1 singlet or the Γ_3 doublet should be the ground state in each of these compounds. Since both Γ_1 and Γ_3 are nonmagnetic, long-range magnetic order does not occur, or ordering is referred to quadrupolar origin. Additional evidence for a distinct CEF influence is superconductivity in both $PrOs_4Sb_{12}$ and $PrRu_4Sb_{12}$, most likely promoted by a nonmagnetic ground state of the Pr ion. Contrary to the above-mentioned materials, the magnetic Γ_5 triplet is supposed to be the ground state in $Pr_{0.73}Fe_4Sb_{12}$, being responsible for a more common type of magnetic order. Although the various Pr-based skutterudites are isoelectronic, physical properties vary significantly among this family of compounds. Harima has shown[37] that the mixing between the electronic states of the various constituents depends on both the pnictogen and the d elements. While d-p mixing is largest in the case of Os-P, it is smallest for Fe-Sb. On the contrary, conduction-electron–f mixing is predominant for Fe-P and is small for Os-Sb. Moreover, the phosphides and the antimonides differ with respect to the density of states at the Fermi energy and the Fermi surface.[28] Varying electronic structures are thus responsible for different CEF effects and a simple point charge model is not applicable for a preliminary calculation of the CEF parameters B_4^0 and B_6^0.

Figures 8 and 9 display the field- and pressure-dependent electrical resistivity of $Pr_{0.73}Fe_4Sb_{12}$. At very low temperatures and low magnetic fields an increase of the electrical resistivity is observed with increasing fields [inset, Fig. 8(a)], but at higher temperatures, externally applied magnetic fields reduce the absolute values of the resistivity.

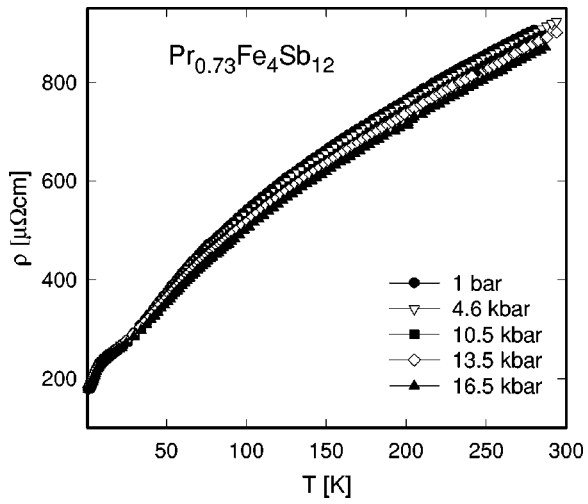

FIG. 9. (a) Temperature- and pressure-dependent electrical resistivity ρ of $Pr_{0.73}Fe_4Sb_{12}$.

In order to analyze features associated with the ordered state, the low-temperature resistivity is accounted for in terms of electron scattering on spin waves, i.e.,

$$\rho = \rho_0 + AT^n \exp(-\Delta/k_B T) \tag{7}$$

(Ref. 38), where ρ_0 represents the residual resistivity, A is a constant, and Δ is an energy gap in the spin-wave energy spectrum. An excitation of a spin wave requires at least the finite energy Δ. Ferromagnetic materials are usually characterized by $n=2$. Least-squares fits according to Eq. (7) are shown as solid lines in the inset of Fig. 8(a). The parameters derived reveal an increase of A, a decrease of n from 1.58 to 0.64, and an increase of Δ from 0.3 to 1.6 K for a field increase from 0 to 5 T, respectively. The values of n neither favor a ferromagnetic nor a Fermi-liquid ground state.

Figure 8(b) shows the isothermal magnetoresistance $\Delta\rho/\rho$ between 2 and 30 K. At low temperatures—well below the phase transition $T_{mag}=4.6$ K—$\Delta\rho/\rho$ smoothly increases up to a maximum of about 3.5% at a magnetic field of 7 T. For higher fields, $\Delta\rho/\rho$ decreases again. With respect to magnetically ordered materials, this particular feature would characterize an antiferromagnet[39] and the maximum in $\Delta\rho/\rho$ represents the field where the system crosses over into a field-induced ferromagnetic state. The decrease of $\Delta\rho/\rho$ at high fields would be in line with the quenching of spin fluctuations, typical for a ferromagnet. Rounding and broadening of the signature at 7 T would then follow from domain wall motion and polycrystalline effects.[39] Contrary to the magnetoresistance, isothermal magnetization does not show a discontinuity around 7 T and $T=2$ K. Tentatively, this inconsistency may be ascribed to different preferred orientations of the various pieces of the polycrystalline material. Strong anisotropy between the $\langle 100\rangle$ and $\langle 111\rangle$ directions has already been reported for single-crystalline $PrFe_4P_{12}$.[16]

Pressure applied to $Pr_{0.73}Fe_4Sb_{12}$ causes a reduction of the absolute resistivity values well above T_{mag} (see Fig. 9). Independent of the magnetic state of the rare earth ion in a certain skutterudite, such a distinct feature is observed in systems where holes dominate the electronic transport. In the case of electron-dominated transport, e.g., in Co-rich ternary skutterudites, the resistivity is found to increase upon increasing pressure.[7,40] In contrast to Eu-filled skutterudites,[7] the present pressure study of Pr revealed no change of the transition temperature, at least within the limit of resolution.

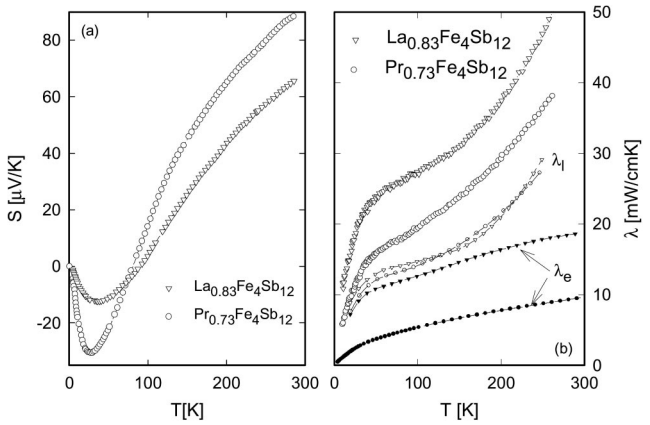

FIG. 10. (a) Temperature-dependent thermopower S of $La_{0.83}Fe_4Sb_{12}$ and $Pr_{0.73}Fe_4Sb_{12}$. (b) Temperature-dependent thermal conductivity of $La_{0.83}Fe_4Sb_{12}$ and $Pr_{0.73}Fe_4Sb_{12}$.

The Seebeck coefficient $S(T)$ of $Pr_{0.73}Fe_4Sb_{12}$ and $La_{0.83}Fe_4Sb_{12}$ is displayed in Fig. 10(a). Common to these compounds and independent of the magnetic state of the rare earth ion is a minimum with negative thermopower and at elevated temperatures a crossover to positive values with little structure up to room temperature. The largest value at room temperature is derived for $Pr_{0.73}Fe_4Sb_{12}$ with $S=88$ μV/K. The positive $S(T)$ values found for these skutterudites indicate holes as principal charge carriers. This can be understood, at least qualitatively, by starting with binary and semiconducting $CoSb_3$. Substituting Co by Fe, holes are created, and a simple carrier count yields four holes in the case of $[Fe_4Sb_{12}]$. Electropositive rare earth ions provide in their trivalent state three conduction electrons that only partly compensate the holes associated with $[Fe_4Sb_{12}]$. The particular degree of compensation depends on the exact amount of rare earth ions filling the voids in the $CoAs_3$ crystal structure. In general and considering a one-band model, absolute $S(T)$ values depend on the carrier density[41] and systems next to the semiconducting state can exhibit giant thermopower values, of the order of several hundred μV/K, while simple metals are characterized by only a few μV/K. The larger values observed for $Pr_{0.73}Fe_4Sb_{12}$, in particular at low temperatures, are attributed to Kondo type interactions that are also reflected by the large C_p/T values of the specific heat. In general, Kondo systems can exhibit enormously large Seebeck coefficients, with a maximum around the characteristic temperature T_K. CEF effects, however, can modify these universal features.[42]

Figure 10(b) shows the temperature-dependent thermal conductivity $\lambda(T)$ of $Pr_{0.73}Fe_4Sb_{12}$ and $La_{0.83}Fe_4Sb_{12}$. $\lambda(T)$ of $Pr_{0.73}Fe_4Sb_{12}$ reaches a value of about 40 mW/cmK at room temperature, which is of the very same magnitude as λ of $LaIrSb_9Ge_3$.[43] The well-characterized series $Ce_y(Fe,Co)_4Sb_{12}$ points at $\lambda(T)$ values ranging at room temperature from 30 to 120 mW/cm K.[44] Note that $\lambda(T)$ as

small as possible, with a magnitude in the proximity of the theoretical lower limit of the thermal conductivity, is considered a prerequisite for a successful use as thermoelectric material.[45] Comparing $\lambda(T)$ of $Pr_{0.73}Fe_4Sb_{12}$ with that of $La_{0.83}Fe_4Sb_{12}$ reveals significantly larger values for the latter. The observed differences are associated with the additional scattering processes of conduction electrons owing to the magnetic moments of the Pr ions. According to Matthiessen's rule, the thermal resistivity increases upon this magnetic interaction and, thus, the overall thermal conductivity reduces.

Taking into account the Wiedemann-Franz law, the total thermal conductivity $\lambda(T)$ can be separated in a standard manner into the electronic part λ_e and the lattice part λ_l. Results are shown in Fig. 10(b) as small solid and open symbols for λ_e and λ_l, respectively. This estimate reveals that the lattice thermal conductivity is of about the same size in the La- and Pr-based compound. Significant differences, however, are obvious for the electronic contribution λ_e. As concluded in the previous paragraph, the lower λ_e values can be associated with the presence of scattering processes of the charge carriers on the Pr magnetic moments. Consequently, the thermal resistivity rises and hence λ_e diminishes.

The figure of merit of $Pr_{0.73}Fe_4Sb_{12}$ at room temperature, based on the displayed measurements of transport coefficients, amounts to about $ZT \approx 0.075$.

IV. SUMMARY

The present study of ternary skutterudite $Pr_{0.73}Fe_4Sb_{12}$ with respect to magnetic properties and transport phenomena reveals magnetic ordering at $T_{mag} \approx 4.6$ K, presumably with some kind of an antiferromagnetic spin arrangement of the Pr^{3+} ions. A value of $\mu_{eff} = 4.19\mu_B$ deduced for $Pr_{0.73}Fe_4Sb_{12}$ may render that the building blocks of the skutterudite structure $[Fe_4Sb_{12}]$ carry an effective magnetic moment of $2.7\mu_B$. The possibility of Fe moments in RFe_4Sb_{12} can be referred to a double-peak structure of the Fe $3d$ DOS in the proximity of the Fermi energy.[28] Such a distinct feature is absent, e.g., in RFe_4P_{12},[27] and thus the iron moment vanishes. Moreover, a significant band broadening of the latter due to a substantially smaller lattice parameter makes an iron moment more unlikely.

Ground-state properties of $Pr_{0.73}Fe_4Sb_{12}$ are primarily determined by crystal field splitting of the $j=4$ total angular momentum. Analyses of the temperature-dependent magnetic susceptibility and electrical resistivity reveal the triplet Γ_5 as ground state, resulting in a magnetic moment of $\mu = 2\mu_B$. Overall CEF splitting is found to be about 215 K. Both specific heat and magnetization data also agree with the set of CEF parameters ($B_4^0 = 0.04$ K and $B_6^0 = 0.001\,33$ K) evaluated. On the contrary, already studied skutterudites based on Pr, e.g., $PrFe_4P_{12}$ or $PrOs_4Sb_{12}$, are characterized by nonmagnetic ground states, i.e., Γ_3 or Γ_1.

Most remarkably, $Pr_{0.73}Fe_4Sb_{12}$ exhibits extraordinary large values of C_p/T at low temperatures, synonymous with large effective masses of the charge carriers. Invoking the resonance level model, usually applied to Kondo systems, revealed a characteristic temperature for fluctuations of about 25 K. A somewhat smaller value was deduced for $Pr_{0.73}Fe_4P_{12}$ ($T_K \approx 9$ K).[16] For the latter, heavy quasiparticles as large as $67m_e$ were found experimentally from de Haas–van Alphen measurements,[15] classifying $Pr_{0.73}Fe_4P_{12}$ as a heavy fermion compound.

Strong electron (hole) correlations are also obvious from the much larger Seebeck coefficient of $Pr_{0.73}Fe_4Sb_{12}$ in comparison with $La_{0.73}Fe_4Sb_{12}$, $Nd_{0.73}Fe_4Sb_{12}$,[46] or $Eu_{0.83}Fe_4Sb_{12}$,[3] making this material promising for thermoelectric applications. In order to further enhance the absolute thermopower values, the number of charge carriers—holes, in this Pr compound—should be reduced without weakening correlation effects. Therefore, studies of Fe/Co and Fe/Ni substitutions in $Pr_{0.73}Fe_4Sb_{12}$ are in progress.

ACKNOWLEDGMENTS

Research was supported by Austrian Grant Nos. FWF-P12899 and P13778 as well as by NEDO (Japan) as an international joint research project. We acknowledge helpful discussions with Dr. Y. Aoki (Tokyo).

[1] I. Shirotani, K. Ohno, C. Sekine, T. Yagi, T. Kawakami, T. Nakanishi, H. Takahashi, J. Tang, A. Matsushita, and T. Matsumoto, Physica B **281-282**, 1021 (2000).

[2] M. E. Danebrock, C. B. H. Evers, and W. Jeitschko, J. Phys. Chem. Solids **57**, 381 (1996).

[3] E. Bauer, St. Berger, A. Galatanu, M. Galli, H. Michor, G. Hilscher, Ch. Paul, B. Ni, M. M. Abd-Elmeguid, V. H. Tran, A. Grytsiv, and P. Rogl, Phys. Rev. B **63**, 224414 (2001).

[4] N. R. Dilley, E. J. Freeman, E. D. Bauer, and M. B. Maple, Phys. Rev. B **58**, 6287 (1998).

[5] N. Takeda and M. Ishikawa, J. Phys.: Condens. Matter **13**, 5971 (2001).

[6] E. Bauer, A. Galatanu, H. Michor, G. Hilscher, P. Rogl, P. Boulet, and H. Noël, Eur. Phys. J. B **14**, 483 (2000).

[7] A. Grytsiv, P. Rogl, St. Berger, Ch. Paul, E. Bauer, C. Godart, B. Ni, M. M. Abd-Elmeguid, A. Saccone, R. Ferro, and D. Kaczorowski, Phys. Rev. B **66**, 094411 (2002).

[8] G. S. Nolas, D. T. Morelli, and T. M. Tritt, Annu. Rev. Mater. Sci. **29**, 89 (1999), and references therein.

[9] I. Shirotani, T. Uchiumi, K. Ohno, C. Sekine, Y. Nakazawa, K. Kanoda, S. Todo, and T. Yagi, Phys. Rev. B **56**, 7866 (1997).

[10] N. Takeda and M. Ishikawa, J. Phys. Soc. Jpn. **69**, 868 (2000).

[11] C. Sekine, T. Uchiumi, I. Shirotani, and T. Yagi, Phys. Rev. Lett. **79**, 3218 (1997).

[12] M. S. Torikachvili, J. W. Chen, Y. Dalichaouch, R. P. Guertin, M. W. McElfresh, C. Rossel, M. B. Maple, and G. P. Meisner, Phys. Rev. B **36**, 8660 (1987).

[13] H. Sato, Y. Abe, H. Okada, T. Matsuda, H. Sugawara, and Y. Aoki, Physica B **281**, 306 (2000).

[14] T. D. Matsuda, H. Okada, H. Sugawara, Y. Aoki, H. Sato, A. V.

Andreev, Y. Shiokawa, V. Sechovsky, T. Honma, E. Yamamoto, and Y. Onuki, Physica B **281-282**, 220 (2000).
[15] H. Sugawara, T. D. Matsuda, K. Abe, K. Aoki, H. Sat, S. Nojiri, Y. Inada, R. Settai, and Y. Onuki, J. Magn. Magn. Mater. **226-230**, 48 (2001).
[16] Y. Aoki, T. Namiki , T. D. Matsuda, K. Abe, H. Sugawara, and H. Sato, Phys. Rev. B **65**, 064446 (2002).
[17] Y. Nakanishi, T. Simizu, M. Yoshizawa, T. Matsuda, H. Sugawara, and H. Sato, Phys. Rev. B **63**, 184429 (2001).
[18] E. D. Bauer, N. A. Frederick, P. C. Ho, V. S. Zapf, and M. B. Maple, Phys. Rev. B **65**, 100506 (2002).
[19] E. Bauer, St. Berger, A. Galatanu, Ch. Paul, M. Della Mea, H. Michor, G. Hilscher A. Grytsiv, P. Rogl, D. Kaczorowski, L. Keller, T. Hermannsdörfer, and P. Fischer, Physica B **312-313**, 842 (2002).
[20] W. Wacha, computer code STRUKTUR, diploma thesis, TU-Vienna, 1989.
[21] A. Leithe-Jasper, D. Kaczorowski, P. Rogl, J. Bogner, M. Reissner, W. Steiner, G. Wiesinger, and C. Godart, Solid State Commun. **109**, 395 (1999).
[22] J. Rodriguez-Carvajal, computer code FULLPROF: A Program for Rietveld Refinement and Pattern Matching Analysis, Abstracts of the Satellite Meeting on Powder Diffraction of the XV Congress International-Union of Crystallography, Talence, France, p. 127.
[23] R. Bachmann, F. J. DiSalvo, T. H. Geballe, R. L. Greene, R. E. Howard, C. N. King, H. C. Kirsch, K. N. Lee, R. E. Schwall, H. U. Thomas, and R. B. Zubeck, Rev. Sci. Instrum. **43**, 205 (1972).
[24] A. Eiling and J. Schilling, J. Phys. F: Met. Phys. **11**, 623 (1981).
[25] W. Jeitschko and D. J. Braun, Acta Crystallogr., Sect. B: Struct. Crystallogr. Cryst. Chem. **33**, 3401 (1977).
[26] E. Bauer (unpublished).
[27] H. Sugawara, Y. Abe, Y. Aoki, H. Sato, M. Hedo, R. Settai, Y. Onuki, and H. Harima, J. Phys. Soc. Jpn. **69**, 2938 (2000).
[28] K. Takegahara and H. Harima, J. Phys. Soc. Jpn. **71**, Suppl., 240 (2002).
[29] J. Sereni, in *Handbook on the Physics and Chemistry of Rare Earths*, edited by K. A. Gschneidner, Jr. and L. Eyring (Elsevier Science, Amsterdam, 1991), Vol. 15.
[30] J. Jensen and A.R. Mackintosh, *Rare Earth Magnetism, Structures and Excitations* (Clarendon Press, Oxford, 1991).
[31] K. Takegahara, H. Harima, and A. Yanase, J. Phys. Soc. Jpn. **5**, 1190 (2001).
[32] E. P. Wohlfart, Rev. Mod. Phys. **25**, 211 (1953).
[33] K. D. Schotte and U. Schotte, Phys. Lett. **55A**, 38 (1975).
[34] M. J. Besnus, A. Braghta, N. Hamdaoui, and A. Meyer, J. Magn. Magn. Mater. **104&107**, 1385 (1992), and references therein.
[35] V. U. S. Rao and W. E. Wallace, Phys. Rev. B **2**, 4613 (1970).
[36] C. Sekine, T. Inaba, K. Kihou, and I. Shirotani, Physica B **281-282**, 300 (2000).
[37] T. Harima (unpublished).
[38] G. T. Meaden, Contemp. Phys. **12**, 313 (1971).
[39] H. Yamada and S. Takada, J. Phys. Soc. Jpn. **34**, 51 (1973).
[40] St. Berger, Ch. Paul, M. Della Mea, E. Bauer, A. Grytsiv, and P. Rogl (unpublished).
[41] C. M. Bhandari and D.M. Rowe, in *CRC Handbook of Thermoelectrics*, edited by D. M. Rowe (CRC Press, Boca Raton, 1995), p. 43.
[42] S. Maekawa, S. Kashiba, and M. Tachiki, J. Phys. Soc. Jpn. **55**, 3194 (1986).
[43] T. M. Tritt, G. S. Nolas, G. A. Slack, A. C. Ehrlich, D. J. Gillespie, and J. L. Cohn, J. Appl. Phys. **79**, 8412 (1996).
[44] G. S. Nolas, J. L. Cohn, and G. A. Slack, Phys. Rev. B **58**, 164 (1998).
[45] G. A. Slack and V. Tsoukala, J. Appl. Phys. **76**, 1665 (1994).
[46] E. Bauer, St. Berger, M. Della Mea, G. Hilscher, H. Michor, Ch. Paul, A. Grytsiv, P. Rogl, E.W. Scheidt, C. Godart, and M. Abd Elmeguid, Acta Phys. Pol. B (to be published).